Practical Classical Molecular Dynamics Simulations for Low-Temperature Plasma Processing: A review

Pascal Brault

Practical Classical Molecular Dynamics Simulations for Low-Temperature Plasma Processing: A review

Pascal Brault

GREMI, CNRS - Université d'Orléans, 14, rue d'Issoudun BP6744, 45067 Orléans Cedex 2, France

July 26, 2023

Abstract

Molecular Dynamics simulations are becoming a powerful tool for examining and predicting atomic and molecular processes in various environment. The present review shows how, in the fields of plasma physics, chemistry and interactions with materials and or liquids, Molecular Dynamics simulations are able to provide significant insights into various processes, among them: gas phase polymerization, deposition, plasma- catalysis, discharge breakdown, vibrational excitation.

Keywords: Molecular Dynamics, Plasma physics, plasma chemistry, plasma-surface interactions, plasma-liquid interactions

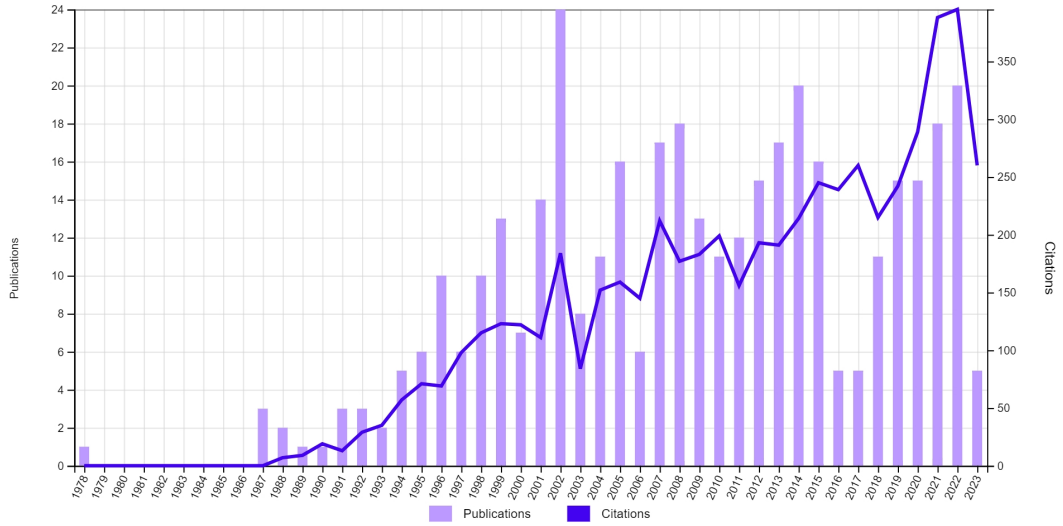

Figure 1: Combined evolution of publication and citation numbers, as reported by Web of Science™ on July 20th, 2023 with after Web of Science using queries ((deposition OR etching) AND ("molecular dynamics")) OR (plasma AND (surfac* or process* or medic* or biolog*) and ("Molecular Dynamics")) with search field "Title"

1 Introduction

Analysing low temperature plasma processes using Molecular Dynamics (MD) simulations started in the mid of 60's - mid of 70's [1, 2, 3, 4]. But it remains marginal, except in the field of dense (warm) plasma. Mid of 80's exhibits an interest of using MD simulations in the field of low-temperature weakly ionized plasma through the study of electron-ion recombination, using MD and Monte-Carlo simulations [5]. But availability of 3- and many-body interatomic potentials, needed for carrying MD simulations, emerged between 1985 and 1990 [6, 7, 8, 9, 10, 11, 12, 13], has really launched the MD simulation approach of plasma etching and deposition. Since the publication of these original articles, many refinements have been made on these forcefields: in Ref [14] are reviewed those always in use at present. The first step for developing MD simulations in low-temperature plasma processes was atom deposition or fast atom deposition mimicking low energy sputtering deposition or ion beam deposition. In the last case ion are treated as fast neutral, considering quick neutralisation of the ion close to the surface [15, 16, 17]. These simulations were often performed in a two dimensional frame due to computer performances at this time. With the advent of 3-body and many-body potentials [14] and availability of High Performance Computers, plasma etching and deposition have been addressed aiming at comparing to and understanding experimental results (see for example pioneering works: [18] and [19, 20]). Despite these progress, around 400 articles, since these pioneering works, have been published (after Web of Science™ using queries ((deposition OR etching) AND ("molecular dynamics")) OR (plasma AND (surfac* or process* or medecine or medic* or biolog*) and ("Molecular Dynamics")) with search field "Title"), with increasing number (around 15 per year) after 1995 but with an accelerated increasing citations after 2015. This shows the growing interest of this simulation technique for plasma processing. Fig 1 displays the combined evolution of publication and citation numbers. The latter reaching 5660.

Nevertheless, it only includes 3 reviews fully dedicated to Molecular Dynamics studies of low-temperature plasma processes [21, 22, 23]. The present review is intended to provide an updated account of the progress of the use of this simulation technique and application to plasmas processing. The next section (Section 2) will address how handling MD simulations and how including experimental conditions for enabling comparison between simulations and experiments, while Section 3 will concern which plasma processes can be described by MD simulations.

2 Practical MD simulations

2.1 Principles

Basically, MD simulations consist in solving the Newton equations of motion for a set of atoms, molecules or particles [24, 25, 26, 27]. Considering a system with N atoms, with coordinates $\{\vec{r}_i\}_{i=1,...,N}$, interaction potential $V = V(\vec{r}_1, \vec{r}_2, ..., \vec{r}_n)$ and m_i being the mass of atom i, The Newton equation reads, at time t:

$$m_i \frac{d^2\vec{r}_i(t)}{dt^2} = \vec{f}_i(t), \quad \text{with} \quad \vec{f}_i(t) = -\frac{\partial V(\vec{r}_1(t), \vec{r}_2(t), ..., \vec{r}_n(t))}{\partial \vec{r}_i(t)} \tag{1}$$

where $\vec{f}_i(t)$ is the force acting on atom i. Moreover, solving Equation (1) amounts determining all trajectories of each individual specie in the considered system. Such a system can be treated with MD for a number of species as large as 10^9, using high performance computing facilities. For solid or liquid systems, this number corresponds to nanoscale sizes : 1 μm of solid or liquid state matter contains around 10^{11} atoms.
Thus, solving Equation (1), "only" requires the knowledge of interaction potentials and a set of two initial conditions, positions and velocities of all species.
Availability of robust semi-empirical interaction potentials allows to run simulations with reasonable computer time, for a given system size and complexity. If not available, quantum chemistry evaluation of the interaction potential can be performed during time integration of the Newton equations of motion. Since the pioneering work[28], many improvements have been elaborated for popularizing Ab-Initio Molecular Dynamics (AIMD, also called First-Principles MD, FPMD) [29]. The most important focus is to have fast and accurate algorithms that overcome the slow computer time inherent to this kind of methods [30]. Last years, Machine Learning approaches have also been developed for providing accurate interactions potentials, leading to faster algorithms than AIMD and being "'universal" such as the very recent M3GNET 3-body potential parametrization [31]. Section 2.4 provides a description of today mostly used interaction potentials. Terminologies like "interaction potentials", "interatomic potentials" and "force fields" will have the same meaning throughout this review.

Besides interaction potentials, the initial conditions are also important for connecting MD simulations to the real world of experiments. The most simple way is to select the initial positions: it may correspond to well defined positions such as crystalline state or can be randomly selected for describing amorphous, liquid or gas phases. For initial velocities, the best way is to randomly select them in "real" distributions such as Maxwell-Boltzmann for thermalized processes, sputtering distributions for sputter deposition [32]. More suitable will be the use of experimental energy distributions obtained by energy resolved mass spectrometry or laser diagnostics.

Last point of attention is the "small" size of the MD simulation boxes that do not allow excess energy dissipation, issued for example from bond formation and or energy transfer to surface of materials or liquids. Indeed, there is not enough species for sharing the excess energy for maintaining the temperature all along the simulations. The solution is the use of thermostats that are setup for absorbing this excess energy in a way consistent with the studied process. Since thermostats are operating over a damping time, it needs to be chosen consistently with realistic energy dissipation time [33] in the experiments [34].

2.2 Relevance for comparison to experiments

The question of comparison with experiments is closely related to which statistical information can be recovered with such small simulations boxes: for comparison a plasma reactor size is ranging from μmeter (micro-plasma) to meter (large plasma materials treatment facilities). For solid and liquid states, there is almost no problem for deriving statistical information (such as diffusion coefficients) since density is of the order of few tens species per nm^3, leading to more than 10000 species per 10x10x10 nm^3 box volume. For gas phase species, the situation is less favourable since at 10^5 Pa (1 atmosphere) pressure, the density is only 2.4 10^{-2}. This requires large box size, i.e. for reaching around 10000 atoms, a 75x75x75 nm^3 volume is required. It should be noticed that even in the case of large interaction potential cutoff length of 2 nm, the simulations will calculate straight trajectories, i.e. without any interactions, for more than 90% of the computer time. Nevertheless, such simulations can be carried out [35]. When going to lower pressure, as those encountered in low-pressure plasma processing, it is necessary to reduce the box size, while keeping the correct description of interactions. For doing this, we can consider that the collision number for a given experiment n_{exp} should be the same in the corresponding MD simulation n_{sim}. In this case, equating

the collision numbers in both situations gives the scaling relation[36]:

$$P_{sim}.d_{sim} = P_{exp}.d_{exp} \tag{2}$$

$d_{exp,sim}$ being the typical experiment and simulation box dimensions, respectively. From Eq. (2) the number of species N_{sim} in the simulation box can be deduced, using $V_{sim} = d_{sim}.S_{sim}$, V_{sim} and S_{sim} being the simulation box volume and basal surface area:

$$N_{sim} = \frac{P_{exp}}{k_B.T_g} S_{sim} d_{exp} \tag{3}$$

Since the goal is to limit the computer time used for calculating straight trajectories without interaction, it is sufficient to have the distance l between species in the simulation box, just greater than the largest interaction cutoff distance r_c of the system. Which leads to:

$$d_{sim} > \frac{N_{sim}}{S_{sim}} r_c^3 \tag{4}$$

which reduces to $d_{sim} > N_{sim}^{1/3} r_c$ for $S_{sim} = d_{sim}^2$. For Coulomb interactions, the cutoff value is the largest short-range cutoff length, when k-space integration is used for the long-range part of the interaction potential. Since low-pressure plasmas are often used for deposition/etching processes, a link between simulated τ_{sim} and experimental τ_{exp} etching/deposition rates can be drawn. In a first attempt, it is enough to consider that sticking coefficients in experiments σ_{exp} and MD simulations σ_{sim} should be the same (equivalently to collision numbers in gas phase). Thus, the experimental rate τ_{exp} can be predicted as:

$$\tau_{exp} = \sigma_{sim}.\phi_{exp} \tag{5}$$

where ϕ_{exp} is the experimental flux of ions of neutrals to the surface.

2.3 Which species, which phenomena ?

Table 1 displays all plasma species that can be treated using MD simulations. It should be pointed out that including electrons in a MD simulations is a problem since its mass is $m_e = 5.45\ 10^{-4}$ amu. And thus sampling interaction potential will require an integration timestep of the equations of motion, in the subattosecond range instead of femtosecond range for heavy species. So including electrons will dramatically increase the computer time. Fortunately, to date, there exists two forcefields that explicitly include electrons: eFF [37, 38] and e-reaxFF [39, 40, 41], which overcome this limitation by setting electron mass to 1 amu. This means the electron is an unreactive negative hydrogen ion. The eFF is mainly used for describing warm dense plasmas while e-reaxFF is used for electron charge transfers in condensed matter and in molecules, and recently for electrical breakdown.

Table 1: Possible included plasma species in MD simulations and associated processes.

Plasma component	inclusion possible ?	Addressed phenomena
atom and hyperthermal specie	yes	deposition, etching
molecule and radical	yes	plasma chemistry, etching, deposition
ions	yes	sputtering, reactivity
electron	yes	Electrical breakdown, e- attachment
photon	yes	polymer degradation, laser sputtering
electric field	yes	e-field assisted processes
electronically excited states	yes	etching
vibrationally excited states	yes	plasma catalysis, dissociative chemisorption

2.4 Interaction Potentials

Many interaction potentials are suitable and employed in molecular dynamics simulations. The most simple ones are pair potential like Lennard-Jones and Morse potentials [42, 43]. Due to their pair nature, they allow very fast

calculations on large systems. But for detailed calculations, there is a need for more accurate interatomic potentials.

For metal atoms, the Embedded Atom Method [12, 13, 44, 45, 46, 47] is a popular many-body forcefield which use the concept of electron (charge) density to describe metallic bonding. Thus, the energy of a solid is a unique functional of the electron density, for which each atom contributes through a spherical, exponentially-decaying field of electron charge, centred at its nucleus, to the overall charge density of the system. Binding of atoms is modelled as embedding these atoms in this "pool" of charge, where the energy gained by embedding an atom, at location r, is some function of the local density. In this frame, the total energy reads:

$$E = \frac{1}{2} \sum_{i,j,i \neq j} \phi_{ij} \left(r_{ij} \right) + \sum_{i} F_i \left(\rho_i \right) \tag{6}$$

where ϕ_{ij} represents the pair energy between atoms i and j at separation r_{ij}, and F_i is the embedding energy associated with embedding an atom i into a position with an electron density ρ_i and functional form $\phi(r)$ reds:

$$\phi(r) = \frac{A \exp\left[-\alpha \left(r/r_e - 1\right)\right]}{1 + \left(r/r_e - \kappa\right)^{20}} - \frac{B \exp\left[-\beta \left(r/r_e - 1\right)\right]}{1 + \left(r/r_e - \lambda\right)^{20}}$$

where r_e is the equilibrium spacing between nearest neighbours, A, B, α, and β are four adjustable parameters, and κ and λ are two additional parameters for the cutoff length. The electron density writes:

$$\rho_i = \sum_{j, j \neq i} f_j \left(r_{ij} \right)$$

with $f_j \left(r_{ij} \right)$ the electron density at atom i due to atom j at distance r_{ij} taking the form:

$$f(r) = \frac{f_e \exp\left[-\beta \left(r/r_e - 1\right)\right]}{1 + \left(r/r_e - \lambda\right)^{20}}.$$

For a pure element a, the EAM potential is thus composed of three functions: the pair energy ϕ, the electron density ρ, and the embedding energy F. For two interacting atoms a and b , the Johnson mixing rule is applied [44], leading to pair potential:

$$\phi^{ab}(r) = \frac{1}{2} \left[\frac{f^b(r)}{f^a(r)} \phi^{aa}(r) + \frac{f^a(r)}{f^b(r)} \phi^{bb}(r) \right]. \tag{7}$$

Embedding energy functions are defines by three equations. For a smooth variation of the embedding energy, these equations are required to match values and slopes at their junctions.

$$F(\rho) = \sum_{i=0}^{3} F_{ni} \left(\frac{\rho}{\rho_n} - 1 \right)^i, \quad \rho < \rho_n, \quad \rho_n = 0.85 \rho_e,$$

$$F(\rho) = \sum_{i=0}^{3} F_i \left(\frac{\rho}{\rho_e} - 1 \right)^i, \quad \rho_n \leqslant \rho < \rho_0, \quad \rho_0 = 1.15 \rho_e,$$

$$F(\rho) = F_e \left[1 - \ln \left(\frac{\rho}{\rho_s} \right)^{\eta} \right] \left(\frac{\rho}{\rho_s} \right)^{\eta}, \quad \rho_0 \leqslant \rho.$$

Extensions of EAM, valid for more systems, known as modified embedded atom method (MEAM) and 2nd nearest-Neighbor MEAM have been proposed [48, 49] for improving accuracy.
These forcefields are widely used for plasma sputtering deposition, nanoparticle growth and plasma treatment of alloyed materials.

When plasma chemistry comes into play, like for plasma polymerisation or grafting [50, 51, 52, 53], plasma-liquid interactions [54], plasma-medicine studies [55, 56, 57], nanoparticle growth in low-temperature plasmas [58, 59], reactive (and variable charge) potentials are needed. Fortunately there are some available suitable forcefields, keeping in mind they are not always highly transferable. Preliminary tests are required for verifying applicability on basic properties of the system under study.

The most simple and faster reactive potential is the Reactive Bond Order Potential (REBO) that has been developed for carbon and hydrocarbon systems [10, 11, 60, 61, 62].

The REBO (Reactive Empirical Bond Order) potentials is an extension of Tersoff potential [7, 8, 9]. The modifications brought by Brenner concern improvements of bond order, repulsive and attractive pair terms. There

are two generation of REBO Potential. In the first generation potential, the total energy of hydrocarbons writes:

$$E = \sum_i \sum_{j(>)i} \left[V_R\left(r_{ij}\right) - \bar{B}_{ij} V_A\left(r_{ij}\right) \right] \tag{8}$$

Where the function $\bar{B}_{ij}, V_R\left(r_{ij}\right)$ and $V_A\left(r_{ij}\right) f_c\left(r_{ij}\right)$ are the bond order, repulsive and attractive potential terms, defined as:

$$\bar{B}_{ij} = \left(b_{ij} + b_{ji}\right)/2 + F_{ij}\left(N_i^{(t)}, N_j^{(t)}, N_{ij}^{(conj)}\right)$$

The interpolation function F_{ij} is used to make the potential continuous, using the cutoff function $f_c(r)$:

$$f_c = \begin{cases} 1 & \text{if } r < R + D \\ \frac{1}{2} - \frac{1}{2}\sin\left[\frac{1}{2}\pi(r-R)/D\right] & \text{if } R - D < r < R + D \\ 0 & \text{if } r > R + D \end{cases}$$

In this way the $N_i^{(t)}$ and $N_j^{(t)}$ which are the number of atoms, respectively, bonded to atom i and j, defined the total number of neighbours. $N_{ij}^{(\text{conj }\!)}$ is the conjugated term of atoms i and j.

$$N_i^{(t)} = \sum_{i(=t)} f_c\left(r_{ij}\right.$$

Full details of each term are described in [11].

Here the repulsive and attractive pair terms with new parameter are given by:

$$V_R\left(r_{ij}\right) = f_{ij}\left(r_{ij}\right) D_{ij}^{(e)} / \left(S_{ij} - 1\right) \exp\left[-\sqrt{2S_{ij}}\beta_{ij}\left(r - R_{ij}^{(e)}\right)\right]$$
$$V_A\left(r_{ij}\right) = f_{ij}\left(r_{ij}\right) D_{ij}^{(e)} S_{ij} / \left(S_{ij} - 1\right) \exp\left[-\sqrt{2/S_{ij}}\beta_{ij}\left(r - R_{ij}^{(e)}\right)\right]$$

The function $f_{ij}(r)$, which restricts the pair potential to nearest neighbours, is given by:

$$f_{ij}(r) = \begin{cases} 1 & \text{if } r < R_{ij}^{(1)} \\ \left[1 + \cos\left[\frac{\pi\left(r - R_{ij}^{(1)}\right)}{\left(R_{ij}^{(2)} - R_{ij}^{(1)}\right)}\right]\right]/2, & \text{if } R_{ij}^{(1)} < r < R_{ij}^{(2)} \\ 0 & \text{if } r > R_{ij}^{(2)} \end{cases}$$

This form makes the correspondence to Morse functions more apparent. If $S_{ij} = 2$, then the pair terms reduce to the usual Morse potential. Furthermore the depth parameter $D_{ij}^{(e)}$, equilibrium distance $R_{ij}^{(e)}$ and β_{ij} are equal to the usual Morse parameters.

Since first generation is not considering the different types of bonding like triple, double or single bonds, the second generation REBO has been developed [60], by introducing a generalization of the bond order function B_{ij}, written as:

$$\bar{B}_{ij} = \frac{1}{2}\left[b_{ij}^{\sigma-\pi} + b_{ji}^{\sigma-\pi}\right] + b_{ji}^{\pi} \tag{9}$$

The functions $b_{ij}^{\sigma-\pi}$ and $b_{ji}^{\sigma-\pi}$ depend on the local coordination and the bond angle for atoms i and j.The function b_{ji}^{π} is further written as:

$$b_{ji}^{\pi} = \prod_{ij}^{RC} + \prod_{ij}^{DH}$$

Where $\prod_{ij}^{RC}$ depend on the bond whether the conjugate bond i and j is a Radical Character. And the term $\prod_{ij}^{DH}$ depend on the dihedral angle for carbon-carbon double bonds. The term $b_{ij}^{\sigma-\pi}$ in Equation (9) is given by:

$$b_{ij}^{\sigma-\pi} = \left[\sum_{k\neq i,j} f_{ik}^{c}\left(r_{ik}\right) G\left(\cos\left(\theta_{ijk}\right)\right) \exp\lambda_{ijk} + P_{ij}\left(N_i^{(C)}, N_j^{(H)}\right)\right]^{-\frac{1}{2}}$$

where f_{ik}^{c} is the cutoff function ensures that the interactions include nearest neighbours only. the function P represents a bicubic spline for interpolation of the potential. $G\left(\cos\left(\theta_{ijk}\right)\right)$ is the angular function. The quantities

$N_i^{(C)}$ and $N_i^{(H)}$ represent the number of carbon and hydrogen atoms for hydrocarbon species, respectively, that are neighbours of atom i. They are defined by sum:

$$N_i^{(C)} = \sum_{k \neq i,j}^{\text{carbon,atoms}} f_{ik}^c \left(r_{ik}\right)$$
$$N_i^{(H)} = \sum_{l \neq i,j}^{\text{hydrogen,atoms}} f_{il}^c \left(r_{il}\right)$$

For more details of the overall functions, which requires a deeper description beyond the scope of this review, the reader is invited to examine the reference [60].

For adding more flexibility and accounting of long range interactions between hydrocarbon species, the 2nd generation REBO potential has been extended by adding a torsional and Lennard-Jones potential, leading to the AIREBO (Adaptive Intermolecular (Reactive Empirical Bond Order) potential. In this case the total AIREBO energy of system is:

$$E = E^{REBO} + E^{LJ} + E^{\text{tors}}$$

Where the term E^{LJ} is the Lennard-Jones potential,contribution in the energy. It ensure the interaction at large distance making AIREBO an intra and inter molecular potential.

E^{tors} is the torsion contribution, needed for studying reactivity of large hydrocarbon molecules.

For going beyond hydrocarbon molecules, two other forcefields have been developed and are among the most used: ReaxFF [63, 64, 65, 66] and COMB (Charge Optimized Many Body) [67, 68, 66]. The bond order is defined as distance dependent, for precisely describing bond formation and breaking. They add the possibility of varying the charge of each atom [69, 70]. Variable charge concept is based on electronegativity equalization following three assumptions: (a) the electronegativity of an atomic site is dependent on the atom's type and charge and is perturbed by the electrostatic potential it is subjected from neighbours (b) charge transfers between atomic sites respect electronegativity equality. (c) The variable charges obey an extended Lagrangian equation in which they have a fictitious mass, velocities, and kinetic energy and then moved with respect to Newtonian mechanics.

In ReaxFF potential, the total energy of a system is given by a summation of all contribution of interaction on the system; this ReaxFF overall system energy is given by [63]:

$$\begin{aligned} E_{\text{system}} =& E_{\text{bond}} + E_{Lp} + E_{\text{over}} + E_{\text{under}} + \\ & E_{\text{val}} + E_{\text{pen}} + E_{\text{coa}} + E_{c_2} + E_{\text{tors}} + \\ & E_{\text{conj}} + E_{H-\text{ bond}} + E_{vd\ \text{Waals}} + E_{\text{Coulomb}} \end{aligned}$$

Where:

E_{bond} is the bond order energy E_{Lp} is the Lone pair energy

E_{over} is overcoordination energy

E_{unde} is undercoordination energy

E_{val} is valence angle term

E_{pen} is penalty energy

E_{coa} is three-body conjugation term

E_{c_2} is Correction for C_2

E_{tors} is torsion angle terms

E_{conj} is four body conjugation term

E_{H-bond} is Hydrogen bond interactions

$E_{vdWaals}$ is van der Waals interactions

E_{coulomb} is Coulomb interaction.

At this step, the focus is on bond order and for saving clarity, the details of the various energy terms are not provided here, but can be found in [63, 64] with a great detail.

The term of bond order energy is the most developed in reaxFF and is a sum of three terms: single bond, double bond and the triple bond. BO_{ij} is defined as:

$$BO_{ij} = BO_{ij}^{\sigma} + BO_{ij}^{\pi} + BO_{ij}^{\pi\pi}$$

Where

$$\begin{aligned} BO_{ij}^{\sigma} &= \exp\left[b_{bo,1}\left(\frac{r_{ij}}{r_0^{\sigma}}\right)^{p_{bo,2}}\right] \\ BO_{ij}^{\pi} &= \exp\left[p_{bo,3}\left(\frac{r_{ij}}{r_0^{\pi}}\right)^{p_{bo,4}}\right] \\ BO_{ij}^{\pi\pi} &= \exp\left[p_{bo,5}\left(\frac{r_{ij}}{r_0^{\pi\pi}}\right)^{p_{bo,6}}\right] \end{aligned} \tag{10}$$

where BO_{ij} is the bond order between atoms i and j, it depends on the local environment. For carbon-carbon interactions, all contributions in set of Equation (10) are used, leading to a max bond order of 3, while for C-H interaction only the σ contribution is used, leading to a maximum bond order of 1 [64].

For COMB family, there are 2 generations COMB [67] and COMB3 [68]. They mainly differ by the atom type involved. It is a similar approach to reaxFF potential, providing with a complementary atom selection. For both reaxFF and COMB(3), there is no predefined molecules but atom assembly connected by interactions that forms (or not) molecule(s). A comparison between these forcefield is available[66].

There are many other forcefields that can be used, either 2-body (pair potentials), 3-body and many-body, reactive or not. It is impossible to include a full list here.

3 MD simulations for plasma processing

It is clear that MD simulations are able to treat interaction between neutral atoms and molecules. It only requires the best forcefield and relevant initial conditions. In plasma, ions are often treated as fast neutral, especially for plasma deposition processes. But the charge can be explicitly given and a charge dependent potential is included. Either the long range is treated in direct space with a large cutoff distance or long range part is treated separately in the k-space. This also requires good forcefields. Reactive variable charge potentials described in Section 2.4 are also usable when necessary, but at expense of higher computer time than other constant charge forcefields. This section will focus on new progress either for processes now tractable by MD simulations or emerging/hot/complex plasma topics

3.1 MD simulations of "new" plasma processes

A way for including plasma effect is the addition of an electric field in the MD simulations. As examples, electric field effects has been studied for monitoring carbon nanotube (CNT) growth [71], pore formation in plasma interaction with phospholipid layers (as encountered in plasma medicine studies) [72].

In the first case, a supported Ni catalyst is exposed to carbon vapour a a given temperature and a constant electric field is applied throughout the deposition process. The CNT growth is thus monitored by this electric field. It is observed that three electric field regimes are effective: weak (1-100 kV.cm^{-1}), medium (500-700 kV.cm^{-1}) and strong (900 kV.cm^{-1}) fields. In the weak field regime the growth is operating through random nucleation as without electric field. In the medium field regime, nucleation is parallel to the electric field vector while for strong field no nucleation on the catalyst occurs, only random bond between carbon atoms. Figure 2 summarizes the CNT growth vs electric field magnitude.

When looking at plasma-medicine/biology applications, introducing electric field in addition to the reactive species (the so-called RONS, Reactive Oxygen and Nitrogen Species [73]) is of paramount importance as demonstrated, for example, by the plasma interaction with phospholipid bilayers (PLB). In this case applying an electric field (0.5 V/nm) results in the formation of pores in the BLP as shown in Figure 3. These pores are expected to facilitate the delivering of ROS (Reactive Oxygen Species) to the PLB, and thus accelerating oxidation and possible damages [72]. Increasing the electric field reduces the formation time of the pores, and thus accelerates the reactivity of ROS with BLP.

Another mechanism, not taken into account until now, has been successfully addressed recently: It is including

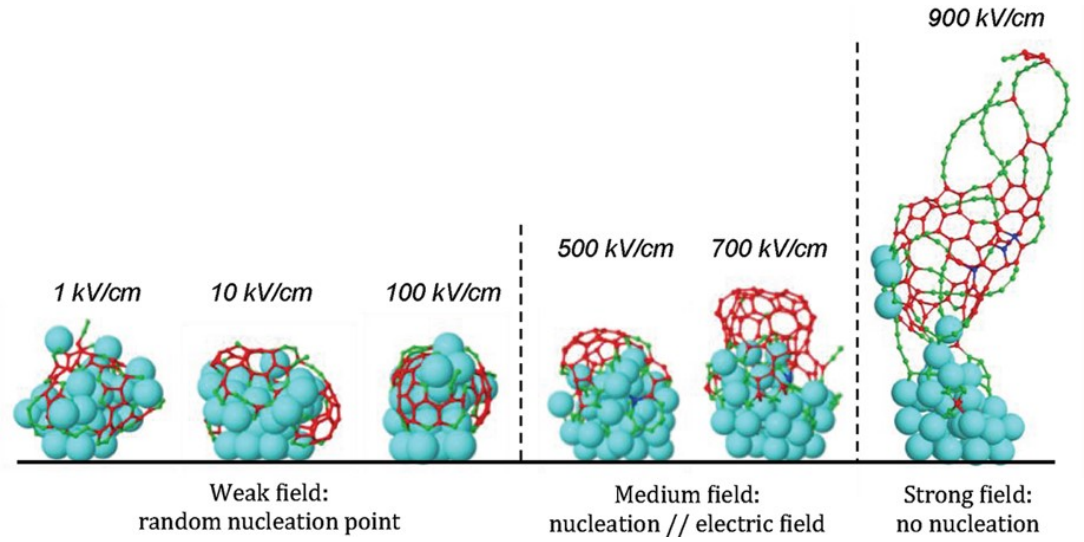

Figure 2: Effect of applying an electric field on the nucleation of a SWNT cap. The small red atoms are 3-coordinated carbon atoms, the small green atoms are 2- or 1-coordinated carbon atoms. The large blue atoms represent nickel atoms. Reprinted with permission from [71]. Copyright 2011 American Chemical Society.

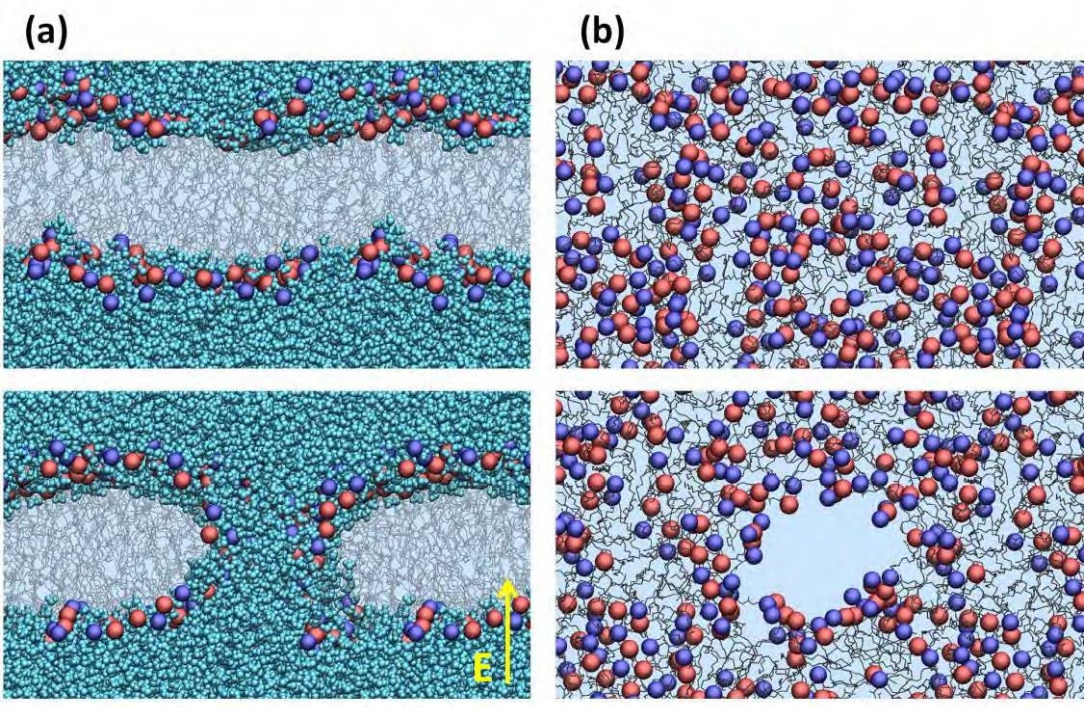

Figure 3: Snapshots from MD simulations, showing the pore formation in a native PLB after $\approx$ 2 ns, upon effect of a constant electric field of 0.5 V.nm^{-1}, (a) side view and (b) top view. The water layers are removed from the top view picture, for the sake of clarity. Reprinted with permission from [72]. Copyright 2017 Elsevier.

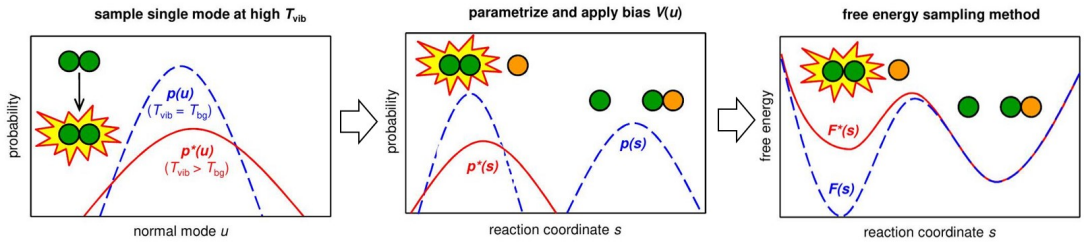

Figure 4: Overview of the principles behind the approach to vibrational excitation. At high T_{vib} , the probability distribution $p^*(\boldsymbol{u})$ along the normal mode differs from the equilibrium distribution $p(\boldsymbol{u})$ at T_{bg}. As a result, the probability distribution along a reaction coordinate $\boldsymbol{s}$ is also affected, which leads to a change in the apparent reaction free energy barrier. In our method, this modified $F^*(\boldsymbol{s})$ (or $p^*(\boldsymbol{s})$) is obtained from a free energy simulation after applying a bias potential $V(\boldsymbol{u})$ that enforces $p^*(\boldsymbol{u})$ at T_{bg}. Adapted with permission from [74]. Copyright 2019 American Chemical Society.

vibrational excitation in MD simulations. Vibrational excitation is a quantum concept. Since there is no vibrational quantum number in classical mechanics, it is not possible to populate and keep vibrational levels in the course of the MD simulations. To circumvent this impossibility, the brilliant idea [74] was to apply a bias potential to the vibrational energy accordingly to the probability distribution at the excited temperature T_{vib}. So the strategy is to model systems in which most modes are in equilibrium with each other at a background temperature (T_{bg}, say 300K for example), while certain selected modes have a (higher) vibrationally excited temperature (T_{vib}). So, probability distribution $p(\vec{R})$ of any system in configuration space at temperature T and potential energy $U(R)$ follows the Boltzmann distribution, used for each two temperatures: $p(\vec{R}) \propto e^{-\frac{U(\vec{R})}{k_B T}}$ which leads to the potential energy surface along the reaction coordinate s, $F(s) = -k_B T \ln p(s) + C$. The change in the potential energy curves is illustrated in Fig. 4.

A remaining major question arising in MD simulations of low temperature plasma is the explicit inclusion of electron motions in Newton equations. If it is widely done in warm dense (plasma) matter through the use of eFF forcefields, which a special case of Wave-packet molecular dynamics [37, 38, 75, 76, 77] or screened potential describing charged particles with ions and atoms [78, 79]. The question for extending the use of this potential, and in which way, in low-pressure low-temperature plasmas, remains opened.

For low pressure low temperature weakly ionized plasmas, the problem lies in the low electron mass, $m_e = 5.45\ 10^{-4}$ amu. When included with heavy atoms, ions, radicals, molecules with $m > 1$ amu, integrating Newton equations of motion would require a very short integration time $dt \approx 10^{-5}$ fs. Thus main computer time will devoted to electron motion in a Coulomb potential, while ions will have a very slow motion. For this reason, reaxFF forcefield, already including variable (Mulliken) charge, has been extended to explicitly include electrons, and is known as e-reaxFF forcefield[39] . Because the fast electron motion still holds, the electron mass m_e is increased to 1 amu (so electron behaves like an unreactive negative hydrogen ion H^-) [39]. Very recently, e-reaxFF was parametrized for allowing description of discharge breakdown between two Silver electrodes separated by an insulating polymer [41] (Figure 5). One electrode is supporting electrons and when running the MD simulation, the electrons migrate towards the counter-electrode as shown in Figure 6, for which trajectories are evolving along void channels between polymer molecules.

Moreover the electric breakdown is shown to occur after a decreasing delay time when increasing applied voltage magnitude. But, effects of considering $m_e = 1$ should be further investigated. It should also kept in mind that using e-reaxFF, with other materials than Silve,r for studying electrical breakdown, requires a new force field parametrization.

This pioneering and breakthrough work open the way to explicitly include electrons in MD simulations in the context of low temperature plasma physics and chemistry, especially for producing high-throughput electron collision data in any situations.

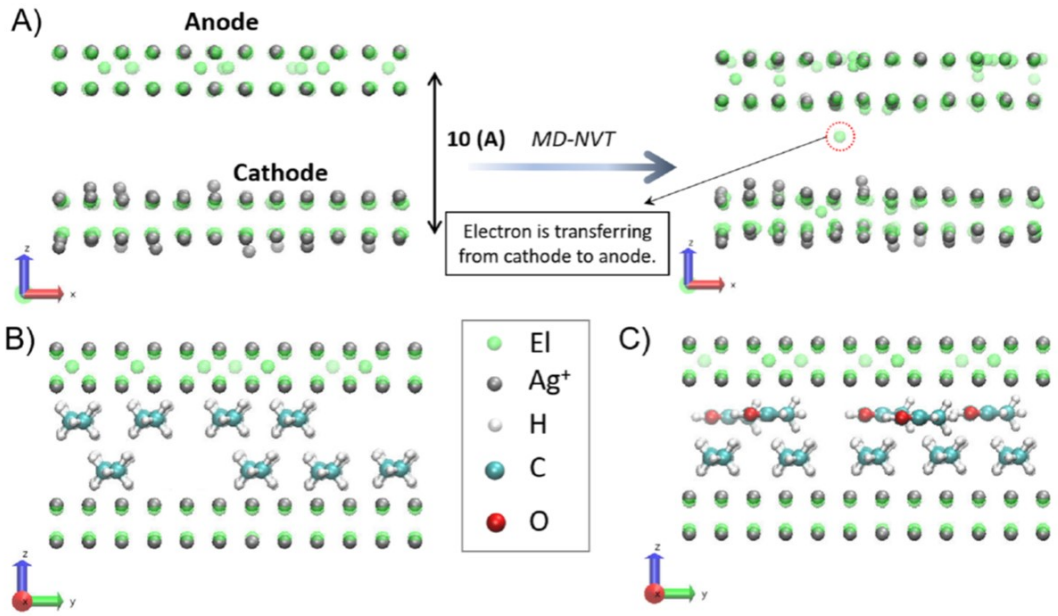

Figure 5: (a) Two 6 × 6 silver slabs including 72 Ag^{+} and 72 electrons. The slabs were separated by 10 Å, and 10 electrons were transferred from the bottom layer to the top layer to apply 40.7 V electric potential to the system. The time that the first electron started transferring from the anode to the cathode is defined as the TDDB. (b) Two silver slabs and eight decane molecules added into the vacuum space between the cathode and the anode. (c) Two silver slabs with five acetophenone and five decane molecules added into the vacuum space between the cathode and the anode. Reprinted with permission from [41]. Copyright 2021 American Institute of Physics.

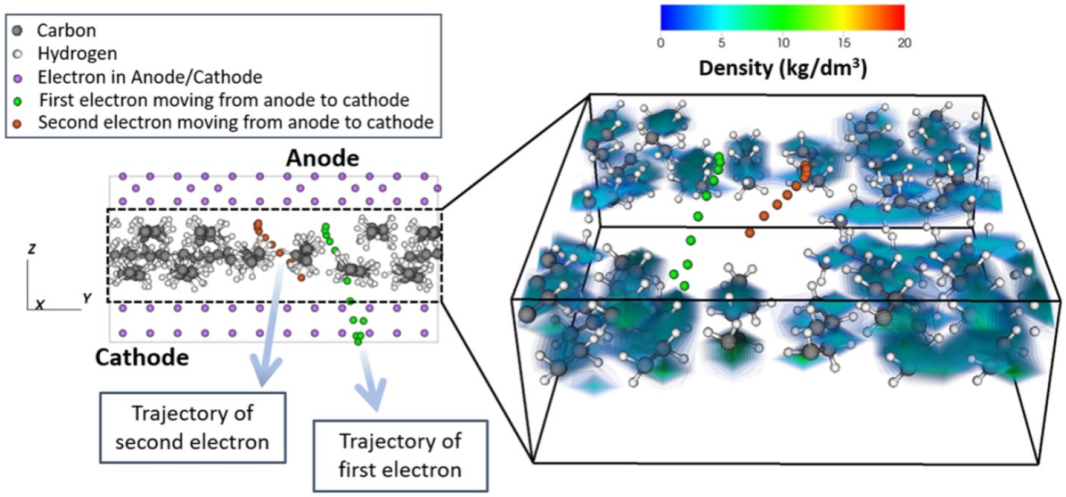

Figure 6: Contour of the system density between the cathode and the anode and the trajectory of the first two electrons transferring from the anode to cathode, indicating that electrons traverse through the voids during the electrical breakdown.. Reprinted with permission from [41]. Copyright 2021 American Institute of Physics.

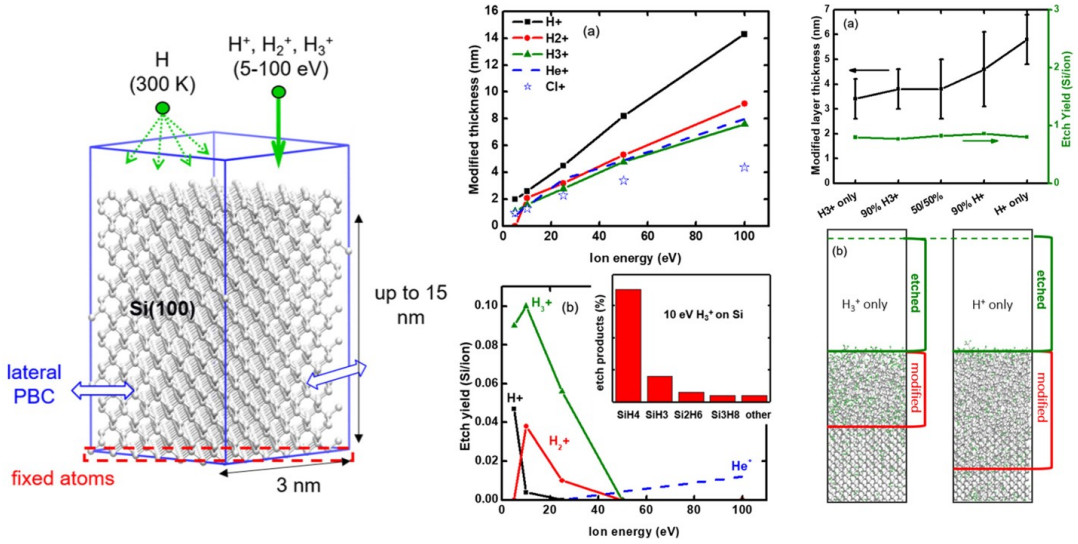

Figure 7: (Left part) Initial (100) c-Si simulation cell used in the MD calculations, (central part) H_x^+ ion bombardment of silicon. (a) Thickness of the modified layer at steady state as a function of the ion energy, for different ion types. Values for pure He^+ [80] and Cl^+ [81] ion bombardment were added for comparison. (b) Etching yields (EY) at steady state as a function of the ion energy, for different ion types. The distribution of etch products for a 10 eV H_3^+ bombardment is shown in the inset graph. (right panel) Mixed H^+ ion/H radical bombardment of Si (ion energy $E_{ion} = 100$ eV, radical to ion flux $\Gamma = 10$) (a) Modified layer thickness and EY, at steady state, as a function of the ion composition. (b) Snapshots of the cells corresponding to the H^+ only and H^+ only cases for an ion dose ≈ 3.5 x 10^{16} ion cm^{-2}. Adapted with permission from [82]. Copyright 2019 Institute of Physics.

3.2 MD simulations for plasma applications

Microelectronics is an historical playground for low-temperature plasma physics and chemistry. It has, without any doubt, driven many progresses in the field. Very recently atomic scale processes have been gain a huge interest due to the miniaturization effort driven by increasing computing performances on smaller and smaller devices. Very recently, an account of atomistic simulation, besides experiments, has been reviewed for almost all processes of microelectronics: etching processes, atomic layer deposition, etc [83]. The level of reachable details is now very impressive. For example, due to available robust and performing interaction potentials, MD simulations of etching processes can be closely connected to experiments. In a recent work [82], etching with H, H^+, H_2^+ and H_3^+ species, is analysed. Especially, when considering Hydrogen ions with different masses, same etch rates are obtained while Silicon affected zone is thicker with low mass ions. Figure 7 summarizes the main features of Hydrogen etching of silicon.

A plasma process which meets more and more interest is High Power Magnetron Sputtering (HiPIMS) deposition, especially for designing complex alloy coatings for many applications [84, 85]. A main feature of HiPIMS is to produce impinging fast metal ions on the surface substrate to be coated. A close comparison of the sputtered ion effects on coatings properties from different plasma sputtering processes and thermal evaporation has been recently reviewed [86, 87]. The main difficulty is to account for the high energy part of sputtered atom energy distribution function. Accounting it as a potential energy allowed to reproduce the main features of deposited films. Moreover, predictions for thermal evaporation and conventional dc sputtering are also well recovering experimental findings. Figures 8 and 9 display the comparison of resulting microstructure of the simulated film deposition for the three processes.

Clearly, HiPIMS process provides the best roughness and film-substrate interface compatible with good adhesion. This also depends on the sputtered ion to neutral ratio.

Further improvement of the method might benefit from using experimental energy resolved high resolution mass spectrometry of both neutral and ions.

Nanoparticle growth is a vast field of applications that magnetron sputtering gas aggregation technique (GAS) is contributing [89, 90, 91, 92]. Basically, sputtering of a target is done in a vapour at enough high pressure ($>$ 10

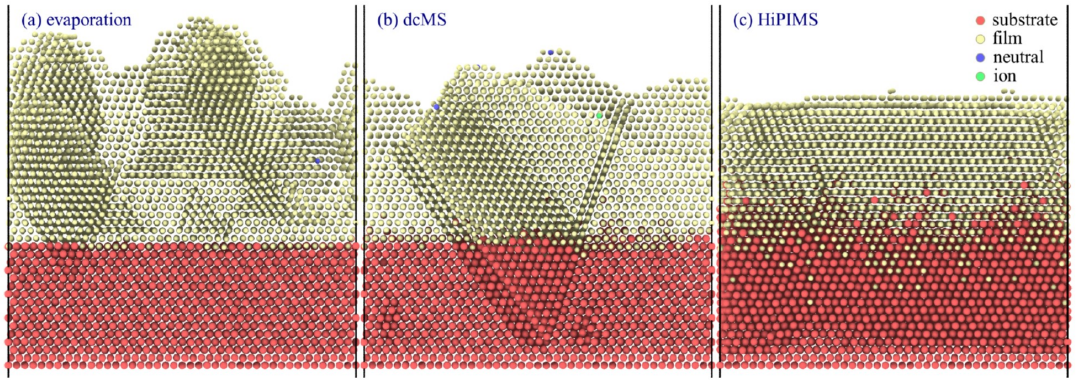

Figure 8: (Illustration of interface mixing using (a) thermal evaporation, (b) dcMS and (c) HiPIMS after 2.5 ns deposition. The red, green, blue and yellow are indicating substrate, neutral, ions and lm atoms.. Reprinted with permission from [86]. Copyright 2019 American Vacuum Society

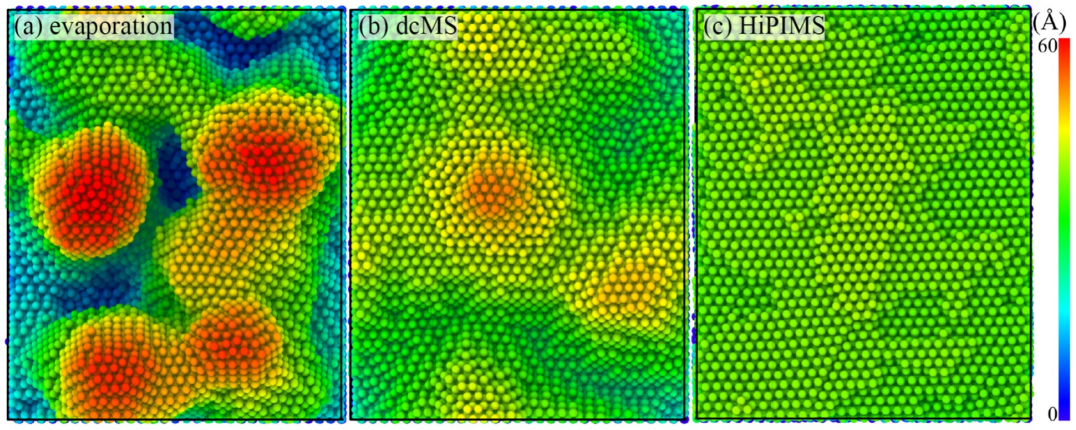

Figure 9: The surface topology obtained using (a) thermal evaporation (b) dcMS and (b) HiPIMS deposition with similar deposition time and energy distribution. The deep blue indicates substrate surface and red denotes thickness higher than 6 nm.. Reprinted with permission from [86]. Copyright 2019 American Vacuum Society

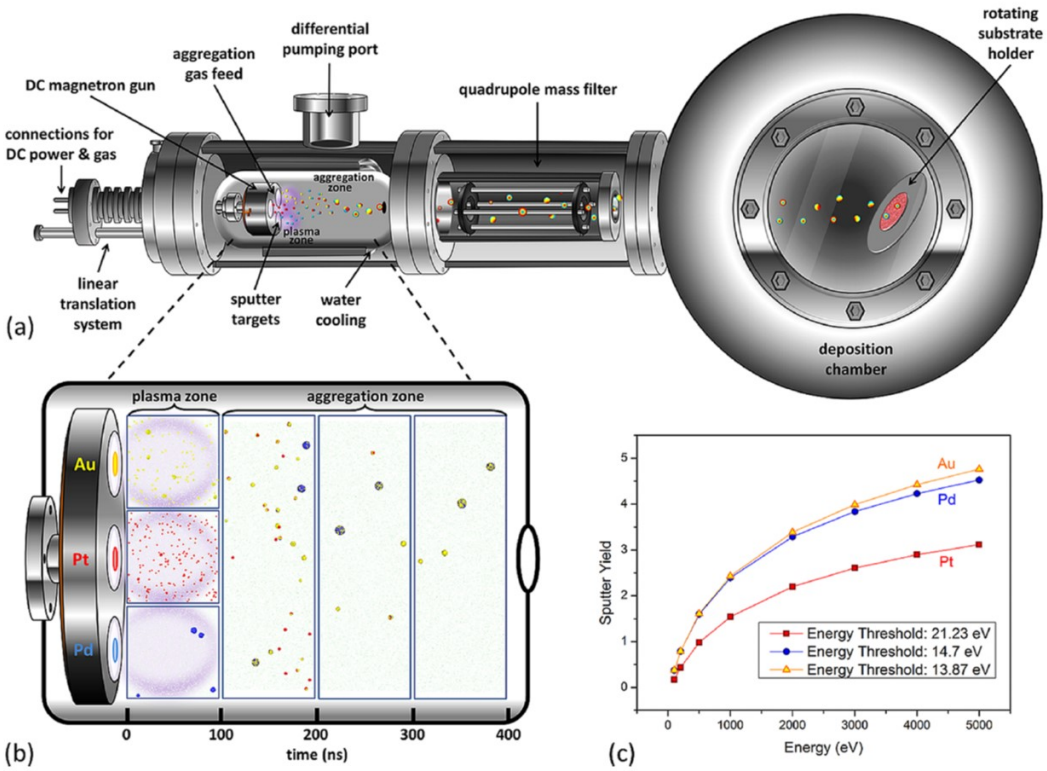

Figure 10: T(a) Schematic representation of a magnetron-sputtering inert-gas-condensation system utilizing a triple-target configuration. (b) Schematic representation of the MD arrangement and its correspondence to the experimental setup. For the first 100 ns, individual nucleation of each element within plasma zones was simulated in a 1000 K Ar gas environment inside 50 × 50 × 50 nm3 simulation boxes. Next, growth within a room temperature aggregation zone represented by a single 150 × 50 × 50 nm3 simulation box was simulated for 300 ns. Au, Pt, Pd, and Ar atoms are represented by yellow, red, blue, and green spheres, respectively. (c) Calculated sputter yields for all three single-element targets for various energies, used as input for MD: Au and Pd have consistently similar yields, whereas the Pt yield is significantly lower, due to its higher sputter energy threshold.. Reprinted from [88]. Open Access data

Pa) so that collisions of sputtered atoms in the vapour allow the gas phase condensation of sputtered atoms as nanoparticles. This atomic process is well suited for MD simulations. Primary attempts, since the pioneering work of Haberland [93] concerned Fe clustering in an Argon gas, thus mimicking gas aggregation [94]. This was followed by modelling alloy nanoparticle growth in GAS for direct comparison with experiments [88, 95, 96]. A relevant procedure is summarized in Figure 10.

Gas phase plasma chemistry is also a nice field for investigating ion - neutral and neutral - neutral reactions. Making use of Equations (2)-(4) allows to well define the simulation box for direct comparison with experiments. The main difficulty is the knowledge of initial composition of the vapour. This can be achieved by experimental mass spectrometry or numerical kinetic/fluid models, as for hydrocarbon plasmas [53]. The dependence of the MD simulation results, i.e. simulated mass spectra, polymerisation mechanisms, on these initial conditions, remains an open question. It certainly requires a large parametric study for classifying MD simulation results along experimental parameters. This will be necessary for assessing a correct comparison with experimental results. The same problem still arises for polymer growth at surfaces: an initial composition does not lead necessarily to a film that corresponds to experiments. The correspondence can unfortunately be unique. When comparing film characterisation, infrared (IR) spectra for example, simulated spectra can reproduce IR peak positions but it is more difficult to obtain peak ratios in agreement with experiments. Here also a parametric MD study is necessary for determining which parameters are affecting the simulated deposited films[51].

Molecular dynamics simulations in the context of Plasma-Liquid interactions [97] is becoming a hot topic where two fields are very active: plasma-medicine/biology [55, 98, 99] and plasma treatment of wastewater [100, 101, 102]. In both cases a first approach is to analyse, via MD simulations, the interactions of ROS, mainly $HO^{\bullet}$, $O^{\bullet}$ with biological materials and organic pollutants molecules in order to predict oxidation reaction pathways and formed products. The key point for such studies is the availability of reactive forcefields. Fortunately the above-mentioned reaxFF is widely used for such studies. Recently, a reaxFF parametrization of organochlorine molecules [103] will broaden the range of emerging pollutant molecules that can be studied using reactive MD simulations. Despite the great success of using reaxFF forcefields, it should noticed, that sometimes reaxFF exhibit energy barrier along reaction coordinates, larger than quantum chemistry predictions [50, 103]. A possible workaround is to increase the operation temperature up to a few additional hundred Kelvin. In this case, care should be taken to the offset value to correctly correlate with experiments, especially when calculating reaction rates.
Since, in both cases, plasma-medicine and wastewater treatment, water is always present, it is advantageous to carry out simulations where interacting species are surrounded by water molecules, preferably at usual water density ($1 g.cm^{-3}$). It can slightly increase computer time, but secondary reactions can be allowed, thus increasing better description of reactions in the real environment.
There at least two approaches, that can be relevant, if direct comparison with experiments is targeted (instead of conducting parametric studies). First of all, creating a simulation box containing a solution with water (or other liquid), the molecule of interest and a number RONS (in agreement with the expected or experimentally available ratio of RONS to this molecule). Then run MD simulation with a temperature ramp for identifying the possible oxidation and degradation products. Thus determining a temperature range realizing a reaction might help for designing the corresponding experimental process[100].
Another way consists in filling the simulation box with water and the molecule of interest and then periodically randomly injecting oxidative radicals (for mimicking RONS delivery to liquid in non-thermal plasma experiments), and identifying degradation products as well as calculating reaction products[104].

4 Conclusion

During the past decade, the use of Molecular Dynamics (classical or ab-initio) has grown for addressing numerous fields of plasma physics and chemistry. The advent of high performance computers, accurate forcefields and easy to use software (the list is too long and is not detailed here), both free and commercial, allow to address complex phenomena as those encountered in plasma volume and/or in interaction with materials and liquids. Almost all processes of plasma can now be described using MD simulations. A recent achievement is including vibrational excitation which opens the way to elucidate numerous mechanisms in the field of plasma catalysis, and more generally

for any applications involving plasma chemistry. Recent explicit inclusion of electrons for describing electric breakdown using reaxFF forcefields gives a great promise of addressing electron-collisions processes in plasma physics. Numerous plasma applications are now accessible using MD simulations since plasma interactions are of atomic and molecular nature. Moreover, MD simulations allow to identify molecular scale mechanisms that impact real process, for example identification of plasma microstructure of deposited films, reaction pathways in plasma chemistry in various area (plasma medicine, plasma treatment of wastewater, etc).

Acknowledgments

I wish to warmly thank all people, either experimentalist, theoreticist or numerician, co-authors and/or colleagues, from GREMI, from France and abroad, being staff members, PhD candidates or postdoc, who contribute by stimulating discussions to the field of Molecular Dynamics simulations in plasma processing: Anne-Lise Thomman, Amaël Caillard, Jean-Marc Bauchire, Johannes Berndt, Eva Kovacevic, Olivier Aubry, Dunpin Hong, Hervé Rabat, Eric Robert, Maxime Mikikian, Lu Xie, Lucile Pentecoste, Soumya Atmane, Mathieu Mougenot, Andrea Jagodar, Sotheara Chuon, Glenn C. Otakantza-Kandjani, Gautier Tetard, Amal Allouch, Matthieu Wolff,Rui Qiu, Fanchao Ye, Jehiel Nteme-Mukunzo, William Chamorro-Coral, Vanessa Orozco-Montes, Sara Ibrahim, Seyedehsara Fazeli, Christine Charles, Rod W. Boswell, David B. Graves, Erik C. Neyts, Monica Magureanu, Corina Bradu, Magda Nistor, Florin Gherendi, Kateb Movaffaq, Tomas Gudmunsson, Sudeep Bhattarcharjee, Christophe Coutanceau, Khaled Hassouni, Armelle Michau, Emilie Despiau Pujo, Tatiana Itina, Germain Valverdu, Marjorie Cavarroc, Pascal Vaudin.

References

[1] R W Hockney. Computer Experiment of Anomalous Diffusion. *The Physics of Fluids*, 9(9):1826–1835, 1966. ISSN 0031-9171. doi: 10.1063/1.1761939. URL `https://doi.org/10.1063/1.1761939`.

[2] Charles K. Birdsall and Dieter Fuss. Clouds-in-clouds, clouds-in-cells physics for many-body plasma simulation. *Journal of Computational Physics*, 3(4):494–511, apr 1969. ISSN 0021-9991. doi: 10.1016/0021-9991(69)90058-8.

[3] R. W. Hockney, S. P. Goel, and J. W. Eastwood. A 10000 particle molecular dynamics model with long range forces. *Chemical Physics Letters*, 21(3):589–591, sep 1973. ISSN 0009-2614. doi: 10.1016/0009-2614(73)80315-X.

[4] R. W. Hockney, S. P. Goel, and J. W. Eastwood. Quiet high-resolution computer models of a plasma. *Journal of Computational Physics*, 14(2):148–158, feb 1974. ISSN 0021-9991. doi: 10.1016/0021-9991(74)90010-2.

[5] Wm. Lowell Morgan. Molecular-dynamics simulation of electron-ion recombination in a nonequilibrium, weakly ionized plasma. *Physical Review A*, 30(2):979–985, aug 1984. ISSN 0556-2791. doi: 10.1103/PhysRevA.30.979. URL `https://link.aps.org/doi/10.1103/PhysRevA.30.979`.

[6] Frank H. Stillinger and Thomas A. Weber. Computer simulation of local order in condensed phases of silicon. *Physical Review B*, 31(8):5262–5271, apr 1985. ISSN 0163-1829. doi: 10.1103/PhysRevB.31.5262. URL `https://link.aps.org/doi/10.1103/PhysRevB.31.5262`.

[7] J. Tersoff. Empirical Interatomic Potential for Carbon, with Applications to Amorphous Carbon. *Physical Review Letters*, 61(25):2879–2882, dec 1988. ISSN 0031-9007. doi: 10.1103/PhysRevLett.61.2879. URL `https://link.aps.org/doi/10.1103/PhysRevLett.61.2879`.

[8] J. Tersoff. New empirical approach for the structure and energy of covalent systems. *Physical Review B*, 37(12):6991–7000, apr 1988. ISSN 0163-1829. doi: 10.1103/PhysRevB.37.6991. URL `https://link.aps.org/doi/10.1103/PhysRevB.37.6991`.

[9] J. Tersoff. Empirical interatomic potential for silicon with improved elastic properties. *Physical Review B*, 38(14):9902–9905, nov 1988. ISSN 0163-1829. doi: 10.1103/PhysRevB.38.9902. URL https://link.aps.org/doi/10.1103/PhysRevB.38.9902.

[10] Donald W. Brenner. Relationship between the embedded-atom method and Tersoff potentials. *Physical Review Letters*, 63(9):1022–1022, aug 1989. ISSN 0031-9007. doi: 10.1103/PhysRevLett.63.1022. URL https://link.aps.org/doi/10.1103/PhysRevLett.63.1022.

[11] Donald W. Brenner. Empirical potential for hydrocarbons for use in simulating the chemical vapor deposition of diamond films. *Physical Review B*, 42(15):9458–9471, nov 1990. ISSN 0163-1829. doi: 10.1103/PhysRevB.42.9458. URL https://link.aps.org/doi/10.1103/PhysRevB.42.9458.

[12] Murray S. Daw and M. I. Baskes. Semiempirical, quantum mechanical calculation of hydrogen embrittlement in metals. *Phys. Rev. Lett.*, 50:1285–1288, Apr 1983. doi: 10.1103/PhysRevLett.50.1285. URL https://link.aps.org/doi/10.1103/PhysRevLett.50.1285.

[13] Murray S. Daw and M. I. Baskes. Embedded-atom method: Derivation and application to impurities, surfaces, and other defects in metals. *Physical Review B*, 29(12):6443–6453, jun 1984. ISSN 0163-1829. doi: 10.1103/PhysRevB.29.6443. URL https://link.aps.org/doi/10.1103/PhysRevB.29.6443.

[14] Susan B. Sinnott and Donald W. Brenner. Three decades of many-body potentials in materials research. *MRS Bulletin*, 37(5):469–473, may 2012. ISSN 08837694. doi: 10.1557/MRS.2012.88/FIGURES/3. URL https://link.springer.com/article/10.1557/mrs.2012.88.

[15] Karl-Heinz Müller. Stress and microstructure of sputter-deposited thin films: Molecular dynamics investigations. *Journal of Applied Physics*, 62(5):1796–1799, 1987. ISSN 0021-8979. doi: 10.1063/1.339559. URL https://doi.org/10.1063/1.339559.

[16] Karl-Heinz Müller. Ion-beam-induced epitaxial vapor-phase growth: A molecular-dynamics study. *Physical Review B*, 35(15):7906–7913, may 1987. ISSN 0163-1829. doi: 10.1103/PhysRevB.35.7906. URL https://link.aps.org/doi/10.1103/PhysRevB.35.7906.

[17] Karl-Heinz Müller. Role of incident kinetic energy of adatoms in thin film growth. *Surface Science*, 184(1-2): L375–L382, may 1987. ISSN 0039-6028. doi: 10.1016/S0039-6028(87)80265-0.

[18] M E Barone and D B Graves. Chemical and physical sputtering of fluorinated silicon. *Journal of Applied Physics*, 77(3):1263–1274, 1995. ISSN 0021-8979. doi: 10.1063/1.358928. URL https://doi.org/10.1063/1.358928.

[19] W. D. Luedtke and Uzi Landman. Molecular-dynamics studies of the growth modes and structure of amorphous silicon films via atom deposition. *Phys. Rev. B*, 40:11733–11746, Dec 1989. doi: 10.1103/PhysRevB.40.11733. URL https://link.aps.org/doi/10.1103/PhysRevB.40.11733.

[20] C. M. Gilmore and J. A. Sprague. Molecular-dynamics simulation of the energetic deposition of ag thin films. *Phys. Rev. B*, 44:8950–8957, Oct 1991. doi: 10.1103/PhysRevB.44.8950. URL https://link.aps.org/doi/10.1103/PhysRevB.44.8950.

[21] F. Gou, A. W. Kleyn, and M. A. Gleeson. The application of molecular dynamics to the study of plasma-surface interactions: Cfx with silicon. *INTERNATIONAL REVIEWS IN PHYSICAL CHEMISTRY*, 27(2): 229–271, 2008. ISSN 0144-235X. doi: 10.1080/01442350801928014.

[22] David B. Graves and Pascal Brault. Molecular dynamics for low temperature plasma-surface interaction studies. *JOURNAL OF PHYSICS D-APPLIED PHYSICS*, 42(19):194011, OCT 7 2009. ISSN 0022-3727. doi: 10.1088/0022-3727/42/19/194011.

[23] E.C. Neyts and P. Brault. Molecular Dynamics Simulations for Plasma-Surface Interactions. *Plasma Processes and Polymers*, 14(1-2):1600145, 2017. ISSN 16128869. doi: 10.1002/ppap.201600145.

[24] James M Haile. *Molecular dynamics simulation: elementary methods*. John Wiley & Sons, Inc., 1992.

[25] D Frenkel and B Smit. *Understanding molecular simulation 2nd edition*. Academic Press, London, UK, 2002.

[26] Dennis C Rapaport. *The art of molecular dynamics simulation*. Cambridge university press, 2004.

[27] Michael P. Allen and Dominic J. Tildesley. *Computer Simulation of Liquids*. Oxford University Press, 06 2017. ISBN 9780198803195. doi: 10.1093/oso/9780198803195.001.0001. URL https://doi.org/10.1093/oso/9780198803195.001.0001.

[28] R. Car and M. Parrinello. Unified Approach for Molecular Dynamics and Density-Functional Theory. *Physical Review Letters*, 55(22):2471–2474, nov 1985. ISSN 0031-9007. doi: 10.1103/PhysRevLett.55.2471. URL https://link.aps.org/doi/10.1103/PhysRevLett.55.2471.

[29] D Marx and J Hutte. *Ab Initio Molecular Dynamics: Theory and Implementation*, volume 22. Publication Series of the John von Neumann Institute for Computing, NIC Series Volume 22, 2004. ISBN 3000056181.

[30] Stefan Grimme, Christoph Bannwarth, and Philip Shushkov. A Robust and Accurate Tight-Binding Quantum Chemical Method for Structures, Vibrational Frequencies, and Noncovalent Interactions of Large Molecular Systems Parametrized for All spd-Block Elements (Z = 1–86). *Journal of Chemical Theory and Computation*, 13(5):1989–2009, apr 2017. doi: 10.1021/acs.jctc.7b00118.

[31] Chi Chen and Shyue Ping Ong. A universal graph deep learning interatomic potential for the periodic table. *Nature Computational Science*, 2(11):718–728, nov 2022. doi: 10.1038/s43588-022-00349-3. URL https://doi.org/10.1038%2Fs43588-022-00349-3.

[32] L. Xie, P. Brault, J.-M. Bauchire, A.-L. Thomann, and L. Bedra. Molecular dynamics simulations of clusters and thin film growth in the context of plasma sputtering deposition. *Journal of Physics D: Applied Physics*, 47(22), 2014. ISSN 13616463 00223727. doi: 10.1088/0022-3727/47/22/224004.

[33] Q. Hou, M. Hou, L. Bardotti, B. Prével, P. Mélinon, and A. Perez. Deposition of Au_N clusters on Au(111) surfaces.I.Atomic-scale modeling. *Physical Review B*, 62(4):2825–2834, jul 2000. ISSN 0163-1829. doi: 10.1103/PhysRevB.62.2825. URL https://link.aps.org/doi/10.1103/PhysRevB.62.2825.

[34] L. Pentecoste, P. Brault, A.-L. Thomann, P. Desgardin, T. Lecas, T. Belhabib, M.-F. Barthe, and T. Sauvage. Low energy and low fluence helium implantations in tungsten: Molecular dynamics simulations and experiments. *Journal of Nuclear Materials*, 470:44–54, 2016. ISSN 00223115. doi: 10.1016/j.jnucmat.2015.12.017.

[35] Swati Swagatika Mishra, Pascal Brault, and Sudeep Bhattacharjee. Molecular dynamics simulations of confined microplasmas at cryogenic temperatures. In Ute Ubert and Sander Nijdam, editors, *ICPIGXXXV Abstract book*, page 118, Egmond aan Zee (NL), 2023. URL https://www.icpig2023.com/home/wiki/942754/book-of-abstracts.

[36] Pascal Brault. Multiscale molecular dynamics simulation of plasma processing: Application to plasma sputtering. *Frontiers in Physics*, 6, 2018. ISSN 2296-424X. doi: 10.3389/fphy.2018.00059. URL https://www.frontiersin.org/articles/10.3389/fphy.2018.00059.

[37] Julius T. Su and William A. Goddard. Excited Electron Dynamics Modeling of Warm Dense Matter. *Physical Review Letters*, 99(18):185003, nov 2007. ISSN 0031-9007. doi: 10.1103/PhysRevLett.99.185003. URL https://link.aps.org/doi/10.1103/PhysRevLett.99.185003.

[38] Andres Jaramillo-Botero, Julius Su, An Qi, and William A. Goddard III. Large-scale, long-term nonadiabatic electron molecular dynamics for describing material properties and phenomena in extreme environments. *Journal of Computational Chemistry*, 32(3):497–512, 2011. doi: https://doi.org/10.1002/jcc.21637. URL https://onlinelibrary.wiley.com/doi/abs/10.1002/jcc.21637.

[39] Md Mahbubul Islam, Grigory Kolesov, Toon Verstraelen, Efthimios Kaxiras, and Adri C. T. van Duin. eReaxFF: A Pseudoclassical Treatment of Explicit Electrons within Reactive Force Field Simulations. *Journal of Chemical Theory and Computation*, 12(8):3463–3472, jul 2016. doi: 10.1021/acs.jctc.6b00432.

[40] Itai Leven, Hongxia Hao, Songchen Tan, Xingyi Guan, Katheryn A. Penrod, Dooman Akbarian, Benjamin Evangelisti, Md Jamil Hossain, Md Mahbubul Islam, Jason P. Koski, Stan Moore, Hasan Metin Aktulga, Adri C. T. van Duin, and Teresa Head-Gordon. Recent Advances for Improving the Accuracy, Transferability, and Efficiency of Reactive Force Fields. *Journal of Chemical Theory and Computation*, 17(6):3237–3251, may 2021. doi: 10.1021/acs.jctc.1c00118.

[41] Dooman Akbarian, Karthik Ganeshan, WH Woodward, Jonathan Moore, and Adri CT Van Duin. Atomistic-scale insight into the polyethylene electrical breakdown: An ereaxff molecular dynamics study. *The Journal of Chemical Physics*, 154(2), 2021.

[42] A. K. Rappé, C. J. Casewit, K. S. Colwell, W. A. Goddard, and W. M. Skiff. UFF, a Full Periodic Table Force Field for Molecular Mechanics and Molecular Dynamics Simulations. *Journal of the American Chemical Society*, 114(25):10024–10035, 1992. ISSN 15205126. doi: 10.1021/ja00051a040.

[43] David W. Jacobson and Gregory B. Thompson. Revisting Lennard Jones, Morse, and N-M potentials for metals. *Computational Materials Science*, 205(February):111206, 2022. ISSN 09270256. doi: 10.1016/j.commatsci.2022.111206. URL `https://doi.org/10.1016/j.commatsci.2022.111206`.

[44] R. A. Johnson. Alloy models with the embedded-atom method. *Physical Review B*, 39 (17):12554–12559, jun 1989. ISSN 0163-1829. doi: 10.1103/PhysRevB.39.12554. URL `https://link.aps.org/doi/10.1103/PhysRevB.39.12554`.

[45] Murray S. Daw, Stephen M. Foiles, and Michael I. Baskes. The embedded-atom method: a review of theory and applications. *Materials Science Reports*, 9(7-8):251–310, mar 1993. ISSN 0920-2307. doi: 10.1016/0920-2307(93)90001-U.

[46] X. W. Zhou, H. N.G. Wadley, R. A. Johnson, D. J. Larson, N. Tabat, A. Cerezo, A. K. Petford-Long, G. D.W. Smith, P. H. Clifton, R. L. Martens, and T. F. Kelly. Atomic scale structure of sputtered metal multilayers. *Acta Materialia*, 49(19):4005–4015, nov 2001. ISSN 1359-6454. doi: 10.1016/S1359-6454(01)00287-7.

[47] X. W. Zhou, R. A. Johnson, and H. N. G. Wadley. Misfit-energy-increasing dislocations in vapor-deposited CoFe/NiFe multilayers. *Physical Review B*, 69(14):144113, apr 2004. ISSN 1098-0121. doi: 10.1103/PhysRevB.69.144113. URL `https://link.aps.org/doi/10.1103/PhysRevB.69.144113`.

[48] M. I. Baskes. Modified embedded-atom potentials for cubic materials and impurities. *Physical Review B*, 46(5):2727–2742, aug 1992. ISSN 0163-1829. doi: 10.1103/PhysRevB.46.2727. URL `https://link.aps.org/doi/10.1103/PhysRevB.46.2727`.

[49] Byeong-Joo Lee and M. I. Baskes. Second nearest-neighbor modified embedded-atom-method potential. *Physical Review B*, 62(13):8564–8567, oct 2000. ISSN 0163-1829. doi: 10.1103/PhysRevB.62.8564. URL `https://link.aps.org/doi/10.1103/PhysRevB.62.8564`.

[50] Mohammad Zarshenas, Konstantin Moshkunov, Bartlomiej Czerwinski, Tom Leyssens, and Arnaud Delcorte. Molecular Dynamics Simulations of Hydrocarbon Film Growth from Acetylene Monomers and Radicals: Effect of Substrate Temperature. *The Journal of Physical Chemistry C*, 122(27):15252–15263, may 2018. doi: 10.1021/acs.jpcc.8b01334.

[51] Pascal Brault, Marisol Ji, Dario Sciacqua, Fabienne Poncin-Epaillard, Johannes Berndt, and Eva Kovacevic. Insight into acetylene plasma deposition using molecular dynamics simulations. *Plasma Processes and Polymers*, 19(1):1–7, 2022. ISSN 16128869. doi: 10.1002/ppap.202100103.

[52] Andrea Jagodar, Johannes Berndt, Erik von Wahl, Thomas Strunskus, Thomas Lecas, Eva Kovacevic, and Pascal Brault. Nitrogen incorporation in graphene nanowalls via plasma processes: Experiments and simulations. *Applied Surface Science*, 591(November 2021):153165, 2022. ISSN 01694332. doi: 10.1016/j.apsusc.2022.153165. URL `https://doi.org/10.1016/j.apsusc.2022.153165`.

[53] Glenn O Kandjani, Pascal Brault, Maxime Mikikian, Gautier Tetard, Armelle Michau, and Khaled Hassouni. Molecular dynamics simulations of reactive neutral chemistry in an argon-methane plasma. *Plasma Processes and Polymers*, 20(4):2200192, 2023. doi: https://doi.org/10.1002/ppap.202200192. URL https://onlinelibrary.wiley.com/doi/abs/10.1002/ppap.202200192.

[54] M Yusupov, E C Neyts, P Simon, G Berdiyorov, R Snoeckx, A C T van Duin, and A Bogaerts. Reactive molecular dynamics simulations of oxygen species in a liquid water layer of interest for plasma medicine. *Journal of Physics D: Applied Physics*, 47(2):025205, jan 2014. ISSN 0022-3727. doi: 10.1088/0022-3727/47/2/025205. URL https://iopscience.iop.org/article/10.1088/0022-3727/47/2/025205.

[55] Annemie Bogaerts, Maksudbek Yusupov, Jonas der Paal, Christof C W Verlackt, and Erik C Neyts. Reactive Molecular Dynamics Simulations for a Better Insight in Plasma Medicine. *Plasma Processes and Polymers*, 11(12):1156–1168, 2014. doi: https://doi.org/10.1002/ppap.201400084. URL https://onlinelibrary.wiley.com/doi/abs/10.1002/ppap.201400084.

[56] Erik C Neyts, Maksudbek Yusupov, Christof C Verlackt, and Annemie Bogaerts. Computer simulations of plasma–biomolecule and plasma–tissue interactions for a better insight in plasma medicine. *Journal of Physics D: Applied Physics*, 47(29):293001, jul 2014. ISSN 0022-3727. doi: 10.1088/0022-3727/47/29/293001. URL https://iopscience.iop.org/article/10.1088/0022-3727/47/29/293001.

[57] Annemie Bogaerts, Narjes Khosravian, Jonas Van Der Paal, Christof C.W. Verlackt, Maksudbek Yusupov, Balu Kamaraj, and Erik C. Neyts. Multi-level molecular modelling for plasma medicine. *Journal of Physics D: Applied Physics*, 49(5):054002, dec 2015. ISSN 0022-3727. doi: 10.1088/0022-3727/49/5/054002. URL https://iopscience.iop.org/article/10.1088/0022-3727/49/5/054002 https://iopscience.iop.org/article/10.1088/0022-3727/49/5/054002/meta.

[58] Giovanni Barcaro, Susanna Monti, Luca Sementa, and Vincenzo Carravetta. Modeling Nucleation and Growth of ZnO Nanoparticles in a Low Temperature Plasma by Reactive Dynamics. *Journal of Chemical Theory and Computation*, 15(3):2010–2021, feb 2019. doi: 10.1021/acs.jctc.8b01222.

[59] P. Brault, W. Chamorro-Coral, S. Chuon, A. Caillard, J.-M. Bauchire, S. Baranton, C. Coutanceau, and E. Neyts. Molecular dynamics simulations of initial Pd and PdO nanocluster growth in a magnetron gas aggregation source. *Frontiers of Chemical Science and Engineering*, 13(2), 2019. ISSN 20950187. doi: 10.1007/s11705-019-1792-5.

[60] Donald W Brenner, Olga A Shenderova, Judith A Harrison, Steven J Stuart, Boris Ni, and Susan B Sinnott. A second-generation reactive empirical bond order (REBO) potential energy expression for hydrocarbons. *Journal of Physics: Condensed Matter*, 14(4):783–802, feb 2002. ISSN 0953-8984. doi: 10.1088/0953-8984/14/4/312. URL https://iopscience.iop.org/article/10.1088/0953-8984/14/4/312.

[61] Boris Ni, Ki-Ho Lee, and Susan B Sinnott. A reactive empirical bond order (REBO) potential for hydrocarbon–oxygen interactions. *Journal of Physics: Condensed Matter*, 16 (41):7261–7275, oct 2004. ISSN 0953-8984. doi: 10.1088/0953-8984/16/41/008. URL https://iopscience.iop.org/article/10.1088/0953-8984/16/41/008.

[62] Alexandre F. Fonseca, Geunsik Lee, Tammie L. Borders, Hengji Zhang, Travis W. Kemper, Tzu-Ray Shan, Susan B. Sinnott, and Kyeongjae Cho. Reparameterization of the REBO-CHO potential for graphene oxide molecular dynamics simulations. *Physical Review B*, 84(7):075460, aug 2011. ISSN 1098-0121. doi: 10.1103/PhysRevB.84.075460. URL https://link.aps.org/doi/10.1103/PhysRevB.84.075460.

[63] Adri C. T. van Duin, Siddharth Dasgupta, Francois Lorant, and William A. Goddard. ReaxFF: A Reactive Force Field for Hydrocarbons. *The Journal of Physical Chemistry A*, 105(41):9396–9409, sep 2001. doi: 10.1021/jp004368u.

[64] Kimberly Chenoweth, Adri C. T. van Duin, and William A. Goddard. ReaxFF Reactive Force Field for Molecular Dynamics Simulations of Hydrocarbon Oxidation. *The Journal of Physical Chemistry A*, 112(5): 1040–1053, jan 2008. doi: 10.1021/jp709896w.

[65] Thomas P Senftle, Sungwook Hong, Md Mahbubul Islam, Sudhir B Kylasa, Yuanxia Zheng, Yun Kyung Shin, Chad Junkermeier, Roman Engel-Herbert, Michael J Janik, Hasan Metin Aktulga, Toon Verstraelen, Ananth Grama, and Adri C T van Duin. The ReaxFF reactive force-field: development, applications and future directions. *npj computational*, 2(1):15011, 2016. ISSN 2057-3960. doi: 10.1038/npjcompumats.2015.11. URL https://doi.org/10.1038/npjcompumats.2015.11.

[66] Tao Liang, Yun Kyung Shin, Yu Ting Cheng, Dundar E. Yilmaz, Karthik Guda Vishnu, Osvalds Verners, Chenyu Zou, Simon R. Phillpot, Susan B. Sinnott, and Adri C.T. Van Duin. Reactive Potentials for Advanced Atomistic Simulations. *Annual Review of Materials Research*, 43: 109–129, jul 2013. ISSN 15317331. doi: 10.1146/ANNUREV-MATSCI-071312-121610. URL https://www.annualreviews.org/doi/abs/10.1146/annurev-matsci-071312-121610.

[67] Tzu-Ray Shan, Bryce D. Devine, Travis W. Kemper, Susan B. Sinnott, and Simon R. Phillpot. Charge-optimized many-body potential for the hafnium/hafnium oxide system. *Physical Review B*, 81(12):125328, mar 2010. ISSN 1098-0121. doi: 10.1103/PhysRevB.81.125328. URL https://link.aps.org/doi/10.1103/PhysRevB.81.125328.

[68] Tao Liang, Tzu Ray Shan, Yu Ting Cheng, Bryce D. Devine, Mark Noordhoek, Yangzhong Li, Zhize Lu, Simon R. Phillpot, and Susan B. Sinnott. Classical atomistic simulations of surfaces and heterogeneous interfaces with the charge-optimized many body (COMB) potentials. *Materials Science and Engineering: R: Reports*, 74(9):255–279, sep 2013. ISSN 0927-796X. doi: 10.1016/J.MSER.2013.07.001.

[69] Anthony K. Rappe and William A. Goddard III. Charge equilibration for molecular dynamics simulations. *The Journal of Physical Chemistry*, 95(8):3358–3363, may 1991. doi: 10.1021/j100161a070.

[70] Steven W Rick, Steven J Stuart, and B J Berne. Dynamical fluctuating charge force fields: Application to liquid water. *The Journal of Chemical Physics*, 101(7):6141–6156, 1994. ISSN 0021-9606. doi: 10.1063/1.468398. URL https://doi.org/10.1063/1.468398.

[71] Erik C. Neyts, Adri C. T. van Duin, and Annemie Bogaerts. Insights in the Plasma-Assisted Growth of Carbon Nanotubes through Atomic Scale Simulations: Effect of Electric Field. *Journal of the American Chemical Society*, 134(2):1256–1260, dec 2011. doi: 10.1021/ja2096317.

[72] M. Yusupov, J. Van der Paal, E. C. Neyts, and A. Bogaerts. Synergistic effect of electric field and lipid oxidation on the permeability of cell membranes. *Biochimica et Biophysica Acta (BBA) - General Subjects*, 1861(4):839–847, apr 2017. ISSN 0304-4165. doi: 10.1016/J.BBAGEN.2017.01.030.

[73] Youssef Morabit, Mohammad I. Hasan, Richard D. Whalley, Eric Robert, Martina Modic, and James L. Walsh. A review of the gas and liquid phase interactions in low-temperature plasma jets used for biomedical applications. *The European Physical Journal D 2021 75:1*, 75(1):1–26, jan 2021. ISSN 1434-6079. doi: 10.1140/EPJD/S10053-020-00004-4. URL https://link.springer.com/article/10.1140/epjd/s10053-020-00004-4.

[74] Kristof M. Bal, Annemie Bogaerts, and Erik C. Neyts. Ensemble-Based Molecular Simulation of Chemical Reactions under Vibrational Nonequilibrium. *The Journal of Physical Chemistry Letters*, 11(2):401–406, dec 2019. doi: 10.1021/acs.jpclett.9b03356.

[75] Yaroslav S Lavrinenko, Igor V Morozov, and Ilya A Valuev. Wave packet molecular dynamics–density functional theory method for non-ideal plasma and warm dense matter simulations. *Contributions to Plasma Physics*, 59(4-5):e201800179, 2019. doi: https://doi.org/10.1002/ctpp.201800179. URL https://onlinelibrary.wiley.com/doi/abs/10.1002/ctpp.201800179.

[76] R. A. Davis, W. A. Angermeier, R. K. T. Hermsmeier, and T. G. White. Ion modes in dense ionized plasmas through nonadiabatic molecular dynamics. *Phys. Rev. Res.*, 2:043139, Oct 2020. doi: 10.1103/PhysRevResearch.2.043139. URL https://link.aps.org/doi/10.1103/PhysRevResearch.2.043139.

[77] Rui Jin, Malik Muhammad Abdullah, Zoltan Jurek, Robin Santra, and Sang-Kil Son. Transient ionization potential depression in nonthermal dense plasmas at high x-ray intensity. *Physical Review E*, 103(2):023203, feb 2021. ISSN 2470-0045. doi: 10.1103/PhysRevE.103.023203. URL https://link.aps.org/doi/10.1103/PhysRevE.103.023203.

[78] T. S. Ramazanov and K. N. Dzhumagulova. Effective screened potentials of strongly coupled semiclassical plasma. *Physics of Plasmas*, 9(9):3758, 2002. ISSN 1070664X. doi: 10.1063/1.1499497.

[79] T. S. Ramazanov, K. N. Dzhumagulova, and M. T. Gabdullin. Effective potentials for ion-ion and charge-atom interactions of dense semiclassical plasma. *Physics of Plasmas*, 17(4):1–7, 2010. ISSN 1070664X. doi: 10.1063/1.3381078.

[80] Vahagn Martirosyan, Emilie Despiau-Pujo, Jerome Dubois, Gilles Cunge, and Olivier Joubert. Helium plasma modification of Si and Si3N4 thin films for advanced etch processes. *Journal of Vacuum Science & Technology A: Vacuum, Surfaces, and Films*, 36(4), jul 2018. ISSN 0734-2101. doi: 10.1116/1.5025152/245647. URL /avs/jva/article/36/4/041301/245647/Helium-plasma-modification-of-Si-and-Si3N4-thin.

[81] Paulin Brichon, Emilie Despiau-Pujo, and Olivier Joubert. MD simulations of low energy Cl x + ions interaction with ultrathin silicon layers for advanced etch processes . *Journal of Vacuum Science & Technology A: Vacuum, Surfaces, and Films*, 32(2):021301, mar 2014. ISSN 0734-2101. doi: 10.1116/1.4827016/985306. URL /avs/jva/article/32/2/021301/985306/MD-simulations-of-low-energy-Clx-ions-interaction.

[82] V. Martirosyan, O. Joubert, and E. Despiau-Pujo. Modification mechanisms of silicon thin films in low-temperature hydrogen plasmas. *Journal of Physics D: Applied Physics*, 52(5), 2019. ISSN 13616463. doi: 10.1088/1361-6463/aaefe0.

[83] Kenji Ishikawa, Tatsuo Ishijima, Tatsuru Shirafuji, Silvia Armini, Emilie Despiau-Pujo, Richard A. Gottscho, Keren J. Kanarik, Gert J. Leusink, Nathan Marchack, Takahide Murayama, Yasuhiro Morikawa, Gottlieb S. Oehrlein, Sangwuk Park, Hisataka Hayashi, and Keizo Kinoshita. Rethinking surface reactions in nanoscale dry processes toward atomic precision and beyond: A physics and chemistry perspective. *Japanese Journal of Applied Physics*, 58(SE), 2019. ISSN 13474065. doi: 10.7567/1347-4065/ab163e.

[84] André Anders. Tutorial: Reactive high power impulse magnetron sputtering (R-HiPIMS). *Journal of Applied Physics*, 121(17):171101, 03 2017. ISSN 0021-8979. doi: 10.1063/1.4978350. URL https://doi.org/10.1063/1.4978350.

[85] Jon Tomas Gudmundsson, Andre Anders, and Achim Von Keudell. Foundations of physical vapor deposition. *Plasma Sources Science and Technology*, page 083001, 2022.

[86] Movaffaq Kateb, Hamidreza Hajihoseini, Jon Tomas Gudmundsson, and Snorri Ingvarsson. Role of ionization fraction on the surface roughness, density, and interface mixing of the films deposited by thermal evaporation, dc magnetron sputtering, and HiPIMS: An atomistic simulation. *Journal of Vacuum Science & Technology A*, 37(3):031306, may 2019. ISSN 0734-2101. doi: 10.1116/1.5094429/910813. URL /avs/jva/article/37/3/031306/910813/Role-of-ionization-fraction-on-the-surface.

[87] Movaffaq Kateb, Jon Tomas Gudmundsson, Pascal Brault, Andrei Manolescu, and Snorri Ingvarsson. On the role of ion potential energy in low energy HiPIMS deposition: An atomistic simulation. *Surface and Coatings Technology*, 426:127726, nov 2021. ISSN 0257-8972. doi: 10.1016/J.SURFCOAT.2021.127726.

[88] Panagiotis Grammatikopoulos, Stephan Steinhauer, Jerome Vernieres, Vidyadhar Singh, and Mukhles Sowwan. Nanoparticle design by gas-phase synthesis. *Advances in Physics: X*, 1(1):81–100, 2016. doi: 10.1080/23746149.2016.1142829. URL https://doi.org/10.1080/23746149.2016.1142829.

[89] C Xirouchaki and R E Palmer. Deposition of size-selected metal clusters generated by magnetron sputtering and gas condensation: a progress review. *Philosophical Transactions of the Royal Society of London. Series A: Mathematical, Physical and Engineering Sciences*, 362(1814):117–124, 2004.

[90] E. Quesnel, E. Pauliac-Vaujour, and V. Muffato. Modeling metallic nanoparticle synthesis in a magnetron-based nanocluster source by gas condensation of a sputtered vapor. *Journal of Applied Physics*, 107(5), mar 2010. ISSN 00218979. doi: 10.1063/1.3310420/907017. URL /aip/jap/article/107/5/054309/907017/Modeling-metallic-nanoparticle-synthesis-in-a.

[91] A Caillard, S Cuynet, T Lecas, P Andreazza, M Mikikian, A-L Thomann, and P Brault. PdPt catalyst synthesized using a gas aggregation source and magnetron sputtering for fuel cell electrodes. *Journal of Physics D: Applied Physics*, 48(47):475302, dec 2015. ISSN 0022-3727. doi: 10.1088/0022-3727/48/47/475302. URL https://iopscience.iop.org/article/10.1088/0022-3727/48/47/475302.

[92] O. Kylián, D. Nikitin, J. Hanuš, S. Ali-Ogly, P. Pleskunov, and H. Biederman. Plasma-assisted gas-phase aggregation of clusters for functional nanomaterials. *Journal of Vacuum Science & Technology A*, 41(2):020802, mar 2023. ISSN 0734-2101. doi: 10.1116/6.0002374/2879219. URL /avs/jva/article/41/2/020802/2879219/Plasma-assisted-gas-phase-aggregation-of-clusters.

[93] Hellmut Haberland, Zinetulla Insepov, and Michael Moseler. Molecular-dynamics simulation of thin-film growth by energetic cluster impact. *Physical Review B*, 51(16):11061–11067, apr 1995. ISSN 0163-1829. doi: 10.1103/PhysRevB.51.11061. URL https://link.aps.org/doi/10.1103/PhysRevB.51.11061.

[94] N Lümmen and T Kraska. Investigation of the formation of iron nanoparticles from the gas phase by molecular dynamics simulation. *Nanotechnology*, 15(5):525–533, may 2004. ISSN 0957-4484. doi: 10.1088/0957-4484/15/5/021. URL https://iopscience.iop.org/article/10.1088/0957-4484/15/5/021.

[95] Pascal Brault, Christophe Coutanceau, Amaël Caillard, and Stève Baranton. Pt3MeAu (Me = Ni, Cu) Fuel Cell Nanocatalyst Growth, Shapes, and Efficiency: A Molecular Dynamics Simulation Approach. *The Journal of Physical Chemistry C*, 123(49):29656–29664, nov 2019. doi: 10.1021/acs.jpcc.9b06476.

[96] Jean-Gabriel Mattei, Panagiotis Grammatikopoulos, Junlei Zhao, Vidyadhar Singh, Jerome Vernieres, Stephan Steinhauer, Alexander Porkovich, Eric Danielson, Kai Nordlund, Flyura Djurabekova, and Mukhles Sowwan. Gas-Phase Synthesis of Trimetallic Nanoparticles. *Chemistry of Materials*, 31(6):2151–2163, mar 2019. doi: 10.1021/acs.chemmater.9b00129.

[97] Patrick Vanraes and Annemie Bogaerts. Plasma physics of liquids—A focused review. *Applied Physics Reviews*, 5(3):031103, jul 2018. ISSN 19319401. doi: 10.1063/1.5020511. URL https://aip.scitation.org/doi/abs/10.1063/1.5020511.

[98] Maksudbek Yusupov, Erik C Neyts, Christof C Verlackt, Umedjon Khalilov, Adri C T van Duin, and Annemie Bogaerts. Inactivation of the Endotoxic Biomolecule Lipid A by Oxygen Plasma Species: A Reactive Molecular Dynamics Study. *Plasma Processes and Polymers*, 12(2):162–171, 2015. doi: https://doi.org/10.1002/ppap.201400064. URL https://onlinelibrary.wiley.com/doi/abs/10.1002/ppap.201400064.

[99] Zihao Yang, Ao Xiao, Dawei Liu, Qi Shi, and Yan Li. Damage of SARS-CoV-2 spike protein by atomic oxygen of cold atmospheric plasma: A molecular dynamics study. *Plasma Processes and Polymers*, 20(7):2200242, 2023. doi: https://doi.org/10.1002/ppap.202200242. URL https://onlinelibrary.wiley.com/doi/abs/10.1002/ppap.202200242.

[100] Pascal Brault, Mado Abraham, Aïda Bensebaa, Olivier Aubry, Dunpin Hong, Hervé Rabat, and Monica Magureanu. Insight into plasma degradation of paracetamol in water using a reactive molecular dynamics approach. *Journal of Applied Physics*, 129(18), 2021. ISSN 10897550. doi: 10.1063/5.0043944.

[101] Mohammad Noor Ghasemi, Feridun Esmaeilzadeh, Dariush Mowla, and Abbas Elhambakhsh. Treatment of methyldiethanolamine wastewater using subcritical and supercritical water oxidation: parameters study, process optimization and degradation mechanism. *Environmental Science and Pollution Research*, 29(38): 57688–57702, 2022. doi: 10.1007/s11356-022-19910-8.

[102] Kunrong Zeng, Kadda Hachem, Mariya Kuznetsova, Supat Chupradit, Chia Hung Su, Hoang Chinh Nguyen, and A. S. El-Shafay. Molecular dynamic simulation and artificial intelligence of lead ions removal from aqueous solution using magnetic-ash-graphene oxide nanocomposite. *Journal of Molecular Liquids*, 347:118290, feb 2022. ISSN 0167-7322. doi: 10.1016/J.MOLLIQ.2021.118290.

[103] Matthieu Wolf, Didier Bégué, and Germain Salvato Vallverdu. Development of a novel ReaxFF reactive potential for organochloride molecules. *Journal of Chemical Physics*, 157(18), nov 2022. ISSN 10897690. doi: 10.1063/5.0120831/2842051. URL /aip/jcp/article/157/18/184302/2842051/Development-of-a-novel-ReaxFF-reactive-potential.

[104] Pascal Brault, Florin Bilea, Monica Magureanu, Corina Bradu, Olivier Aubry, Hervé Rabat, and Dunpin Hong. Plasma degradation of water organic pollutants: Ab-initio molecular dynamics simulations and experiments. *Plasma Processes and Polymers*, page accepted, 2023.